DALTON

Structural variations in nickel(II) and copper(II) MN_4 Schiff-base complexes with deprotonated tetradentate *N,N'*-bis(5-aminopyrazol-4-ylmethylene)polymethylenediamine ligands†

Alexander L. Nivorozhkin,*[a,b] Hans Toftlund,[a] Per Lauge Jørgensen[a] and Leonid E. Nivorozhkin[b]

[a] *Department of Chemistry, Odense University, DK-5230 Odense M, Denmark*
[b] *Institute of Physical and Organic Chemistry, Rostov State University, 344104 Rostov on Don, Russia*

Two series of copper(II) and nickel(II) complexes $[ML^1]$–$[ML^6]$ containing deprotonated tetradentate *N,N'*-bis(5-aminopyrazol-4-ylmethylene)polymethylene diamine ligands L^1–L^6 with varying *n* (2–4) of the bridge $-HC{=}N(CH_2)_nN{=}CH-$ have been prepared and investigated by ^1H NMR, UV/VIS and ESR spectroscopy and cyclic voltammetry measurements. Complexes $[CuL^4]$–$[CuL^6]$ display a gradual alteration of the configuration at the metal centre from planar to pseudo-tetrahedral when going from $n = 2$ to 4 as indicated by the variations in their ESR spectral parameters. This was also reflected in the electronic spectra which exhibited a red shift of the ligand-field bands in this series. The nickel(II) complexes with $n = 2$ or 3 possess a planar structure both in solution and in the solid state, whereas in the case of $[ML^6]$ ($n = 4$), diamagnetic in the solid state, a rapid (on the NMR time-scale) equilibrium between planar low-spin ($S = 0$) and tetrahedral high-spin ($S = 1$) forms was found in chloroform solution with 45% of the high-spin species at 331 K. At low temperatures the planar $\rightleftharpoons$ tetrahedral interconversion is not accompanied by $R \rightleftharpoons S$ enantiomerization at the metal centre due to the higher barriers to inversion of the seven-membered metallocycle which was followed at elevated temperatures by coalescence of the diastereotopic NCH_2 and CCH_2 protons. The crystal structure of $[NiL^6]$ [H_2L^6 = *N,N'*-bis(5-amino-1,3-diphenylpyrazol-4-ylmethylene)butane-1,4-diamine] revealed a planar-to-tetrahedral distorted metal configuration with an angle between the N(1)NiN(2) and N(5)NiN(8) planes of 21° and twist-chair conformation of the seven-membered metallocycle. Cyclic voltammetry showed a reversible $Ni^{II} \longrightarrow Ni^{III}$ oxidation at potentials 0.47–0.51 V and irreversible $Cu^{II} \longrightarrow Cu^{I}$ transformations.

Tuning of the geometry around the metal centre in open-chain four-co-ordinate Schiff-base metal–chelate complexes[1] upon variation in the length of the polymethylene chain between the co-ordinated nitrogen atoms has been extensively studied for nickel(II) and copper(II) complexes derived from the imines of vicinal hydroxy(thio) aromatic and heteroaromatic aldehydes with N_2O_2[2] and N_2S_2[3] chromophores. Fewer data[4] are available for the corresponding complexes MN_4 containing a type of chromophore which mimic some structural features of biomolecules.[5] These compounds which represent a structural type intermediate between open-chain and macrocyclic complexes are also of interest for comparison with the ubiquitous tetraaza macrocyclic complexes. The influence of the macrocyclic ring size as determined by the length of N,N-polymethylene chain on the structural features of MN_4 complexes was recently demonstrated by Lippard and co-workers[6,7] for tetraaza tropocoronand complexes of nickel(II) and copper(II) containing two $N(CH_2)_mN$ bridging fragments with a geometry varying from planar to pseudo-tetrahedral on going from 14- ($m = 2$) to 20-membered ($m = 6$) macrocyclic rings. However, these studies were limited mainly to the crystal structure determination and very little of the spectral features and physicochemical data were reported.

We report here on the synthesis and study of novel dianionic nickel(II) and copper(II) complexes ML based on the tetradentate bis(pyrazolea)diimine ligands H_2L to probe the influence of the polymethylene bridge length *n* on the structural and spectral properties of these complexes having a MN_4 chromophore.

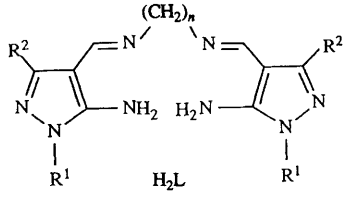

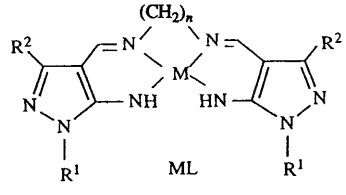

	n	R^1	R^2
$[ML^1]$	2	Me	Ph
$[ML^2]$	3	Me	Ph
$[ML^3]$	4	Me	Ph
$[ML^4]$	2	Ph	Ph
$[ML^5]$	3	Ph	Ph
$[ML^6]$	4	Ph	Ph

Experimental

Physical measurements

Proton NMR spectra were recorded on 250 MHz Bruker AC FT and 300 MHz Varian Unity-300 spectrometers equipped

† *Non-SI unit employed:* $\mu_B \approx 9.27 \times 10^{-24}$ J T^{-1}.

with a variable-temperature probe, ESR spectra using a Varian E-Line Centuries Series X-band frequency instrument at 77 K, infrared spectra on a Perkin-Elmer 580 instrument and electronic spectra with a Shimadzu UV-3100 spectrophotometer. Magnetic susceptibilities in the solid state were determined by the Faraday method and in solution by the Evans method.[8] The molar susceptibilities were corrected for ligand diamagnetism using Pascal's constants.[9] The cyclic voltammetry measurements were performed in dimethylformamide (dmf) (Aldrich, spectroscopic grade, dried over molecular sieves 4 Å and degassed) with tetrabutylammonium perchlorate as supporting electrolyte. A three-electrode system was used in which the working and counter electrodes were platinum and a standard calomel electrode was used as the reference. Microanalyses were carried out by Copenhagen University.

Synthesis of H_2L

***N,N'*-Bis(5-amino-1-methyl-3-phenylpyrazol-4-ylmethylene)-ethane-1,2-diamine H_2L^1.** To a solution of 5-amino-1-methyl-3-phenylpyrazole-4-carbaldehyde[10] (2.0 g, 10 mmol) in Pr^iOH (20 cm^3) was added 1,2-diaminoethane (0.31 g, 5 mmol) and the reaction mixture heated at reflux for 4 h. After evaporation of solvent *in vacuo* the oily residue was recrystallized from aqueous ethanol to give a practically colourless solid after standing in a refrigerator for several days. Yield 1.22 g (62%), m.p. 186 °C (Found: C, 67.5; H, 6.05; N, 26.4. $C_{24}H_{26}N_8$ requires C, 67.6; H, 6.1; N, 26.3%); $\delta_H(CDCl_3)$ 2.29 (s, 6 H, $2CH_3$), 3.76 (s, 4 H, $2CH_2$), 5.70 (br s, 4 H, $2NH_2$), 7.26–7.56 (m, 10 H, 2Ph) and 8.26 (s, 2 H, 2CH=N); $\tilde{\nu}_{max}/cm^{-1}$ (KBr) 3420 (NH_2) and 1598 (C=N).

The compounds H_2L^3–H_2L^6 were prepared according to the above method in 60–70% yields. The samples of H_2L^2 gave unsatisfactory analytical results and always contained an amount of the starting aminoaldehyde. 5-Amino-1,3-diphenylpyrazole-4-carbaldehyde required for the syntheses of H_2L^4–H_2L^6 was obtained[11] analogously to that used above. Yield 70%, m.p. 95 °C (Found: C, 68.3; H; 4.8; N, 14.9. $C_{16}H_{13}N_3O$ requires C, 68.8; H, 4.7; N, 15.0%); $\delta_H(CDCl_3)$ 7.11–7.78 (m, 12 H, 2Ph and NH_2) and 9.79 (s, 1 H, CHO); $\tilde{\nu}_{max}/cm^{-1}$ (KBr) 3428, 3312 (NH_2) and 1646 (CHO).

***N,N'*-Bis(5-amino-1-methyl-3-phenylpyrazol-4-ylmethylene)-butane-1,4-diamine H_2L^3.** M.p. 114 °C (Found: C, 65.3; H, 6.6; N, 23.7. $C_{26}H_{30}N_8 \cdot 1.5H_2O$ requires C, 64.9; H, 6.9; N, 23.3%); $\delta_H(CDCl_3)$ 1.73 [t, *J*(HH) 3.8, 4 H, $2CCH_2$], 2.30 (s, 6 H, $2CH_3$), 3.53 [t, *J*(HH) 3.8 Hz, 4 H, $2NCH_2$], 4.25 (br s, 4 H, $2NH_2$), 7.32–7.55 (m, 10 H, 2Ph) and 8.24 (s, 2 H, 2CH=N).

***N,N'*-Bis(5-amino-1,3-diphenylpyrazol-4-ylmethylene)ethane-1,2-diamine H_2L^4.** M.p. 207 °C (Found: C, 72.1; H, 5.5; N, 20.2. $C_{34}H_{30}N_8 \cdot H_2O$ requires C, 71.8; H, 5.7; N, 19.7%); $\delta_H(CDCl_3)$ 3.77 (s, 4 H, $2CH_2$), 5.80 (br s, 4 H, $2NH_2$), 7.29–7.64 (m, 20 H, 4Ph) and 8.40 (s, 2 H, 2CH=N).

***N,N'*-Bis(5-amino-1,3-diphenylpyrazol-4-ylmethylene)-propane-1,3-diamine H_2L^5.** M.p. 84 °C (Found: C, 73.0; H, 5.7; N, 18.7. $C_{35}H_{32}N_8 \cdot 0.5H_2O$ requires C, 73.3; H, 5.8; N, 19.5%); $\delta_H(CDCl_3)$ 2.00 [qnt, *J*(HH) 6.6, 2 H, CCH_2], 3.61 [t, *J*(HH) 6.6 Hz, 4 H, $2NCH_2$], 5.75 (br s, 4 H, $2NH_2$), 7.33–7.70 (m, 20 H, 4Ph) and 8.43 (s, 2 H, 2CH=N).

***N,N'*-Bis(5-amino-1,3-diphenylpyrazol-4-ylmethylene)-butane-1,4-diamine H_2L^6.** M.p. 156 °C (Found: C, 68.0; H, 6.0; N, 17.7. $C_{36}H_{34}N_8 \cdot 3H_2O$ requires C, 68.3; H, 6.4; N, 17.7%); $\delta_H(CDCl_3)$ 1.73 [t, *J*(HH) 3.7, 4 H, $2CCH_2$], 3.54 [t, *J*(HH) 3.7 Hz, 4 H, $2NCH_2$], 5.80 (br s, 4 H, $2NH_2$), 7.33–7.74 (m, 20 H, 4Ph) and 8.41 (s, 2 H, 2 CH=N).

Synthesis of complexes

Complexes ML were prepared by the reaction of ligands H_2L with metal acetates (*a*) or by the template condensation of aminoaldehydes with metal acetates and diamines (*b*). The two methods gave identical results.

(*a*) To a solution of H_2L (10 mmol) in ethanol (2 cm^3) was added a solution of the metal acetate in ethanol (1 cm^3) and the reaction mixture was heated to reflux for 5 min. The resulting crystals were filtered off and washed with ethanol. Yield 70–80%.

(*b*) To a stirred solution of the corresponding *o*-aminoaldehyde (10 mmol) in ethanol (2 cm^3) were added diamine (5 mmol) and solution of the metal acetate (5 mmol) in ethanol (1 cm^3). The mixture was heated to reflux for 15 min. The precipitate formed was filtered off and washed with ethanol. Yield 70–80%.

The analytical data for ML are listed in Table 1.

Crystallography

Deep brown crystals of [NiL[6]] suitable for single-crystal X-ray diffraction were grown by slow diffusion of ethanol into a saturated chloroform solution of the complex. Diffraction data were collected with a Syntex $P2_1$ diffractometer using graphite-monochromated Mo-Kα radiation. Crystal data and details of the data collection are given in Table 2. The intensity data were corrected for Lorentz and polarization effects and for absorption (using the program DIFABS[12a] after a full isotropic refinement, transmission factors 0.81–1.00). The structure was solved using the program SHELXS 86[12b] and refined (on F^2) by full-matrix least-squares methods using SHELXL 93.[12c] All non-hydrogen atoms were refined anisotropically. The positions of hydrogen atoms were generated geometrically [*d*(C–H) 0.96 Å] except those at N(1) and N(8) obtained from the Fourier-difference synthesis and refined with fixed thermal parameters. Atomic coordinates are listed in Table 3 and selected bond lengths and angles in Table 4. The view of the molecule is shown in Fig. 1.

Complete atomic coordinates, bond lengths and angles have been deposited at the Cambridge Crystallography Data Centre. See Instructions for Authors, *J. Chem. Soc., Dalton Trans.*, 1996, Issue 1.

Results and Discussion

Synthesis of H_2L and metal complexes

The compounds H_2L were prepared by the reaction of 5-amino-4-formylpyrazoles with diamines in 2:1 ratio. Unlike the facile synthesis of Schiff-bases from *o*-aminobenzaldehyde this required a longer reaction time which may be explained by a lower reactivity of the aldehyde group.[13] The ^1H NMR spectra of H_2L display a broad signal of the amino group at δ 4.2–5.8 and a sharp singlet at δ 8.2–8.4 belonging to the CH=N group. The stretching vibrations of the NH_2 group were detected in the IR spectra at 3370–3440 cm^{-1} and those of the CH=N groups in the ranges 1593–1597 and 1619–1625 cm^{-1}. The present study does not provide any conclusive evidence in favour of the *syn* conformation corresponding to the mutual orientation of the amino and aldimino groups as shown in the structural formulae. Alternatively, an *anti* geometrical isomer could be formed by rotation of the aldimino group by 120° around the C_{pz}–CN bond. However, dipole-moment measurements conducted for similar compounds may suggest[14] a preferred occurrence of the *syn* conformation stabilized by a weak intramolecular hydrogen bond $NH_2 \cdots N{=}CH$.

The reaction of nickel(II) and copper(II) acetates with H_2L in ethanol or a template condensation of the aminoaldehydes, metal acetates and diamines yields the complexes ML as was confirmed by the analytical and spectral data. We were unable

Table 1 Analytical data for ML complexes

Complex	M.p./°C	IR[a]/cm^{-1} NH	IR[a]/cm^{-1} CH=N	Analysis (%)[b] C	H	N
[NiL^1]	335	3383	1620, 1596	59.9 (59.65)	5.1 (5.0)	23.1 (23.2)
[CuL^1]	312	3380	1620, 1597	58.8 (59.0)	4.95 (5.0)	22.8 (23.0)
[NiL^2]	286	3379	1625, 1597	60.5 (60.4)	5.4 (5.2)	22.4 (22.5)
[CuL^2]	256	3377	1621, 1597	59.1 (59.8)	5.1 (5.2)	22.3 (22.3)
[NiL^4]	270	3314	1619, 1599	67.5 (67.2)	4.7 (4.65)	18.5 (18.45)
[CuL^4]	277	3388	1619, 1597	66.4 (66.7)	4.5 (4.6)	18.6 (18.3)
[NiL^5]	294	3436	1620, 1597	67.0 (67.65)	4.9 (4.9)	17.9 (19.0)
[CuL^5]	258	3435	1617, 1597	66.8 (67.1)	4.7 (4.8)	17.6 (17.9)
[NiL^6]	244	3436	1615, 1597	66.8 (67.05)	5.15 (5.1)	17.3 (17.6)
[CuL^6]	273	3387	1617, 1593	67.2 (67.5)	5.2 (5.0)	17.3 (17.5)

[a] In KBr. [b] Required values are given in parentheses.

Table 2 Crystal data and details of data collection for the complex [NiL^6]

Formula	$C_{36}H_{32}N_8Ni{\cdot}2CHCl_3$
M	874.14
Crystal size/mm	0.4 × 0.2 × 0.1
Crystal system	Triclinic
Space group	$P\bar{1}$
a/Å	10.149(2)
b/Å	13.890(3)
c/Å	14.528(3)
α/°	76.59(2)
β/°	84.06(2)
γ/°	88.32(2)
U/Å^3	1981.3(7)
D_c/g cm^{-3}	1.456
μ/cm^{-1}	9.3
Z	2
F(000)	896.0
λ/Å	0.7107
Measured reflections	5367
Observed reflections [$I > 2\sigma(I)$]	4153
Scan type	ω–2θ
θ_{max}/°	25
Refined parameters	496
R	0.063
R'[$w = 1/\sigma^2(F_o)$]	0.061
S	1.81

to prepare complexes [ML^3] in an analytically pure form using both methods.

Structure of complex [NiL^6]

The molecule of [NiL^6] has a distorted *cis* square-planar structure. The angle between the N(1)NiN(4) and N(5)NiN(8) planes is 21(1)°. The six-membered metal rings are folded along the N(1)···N(4), N(5)···N(8), N(1)···C(16) and N(8)···C(21) axes. The seven-membered metallocycle adopts a twist-chair conformation with the corresponding dihedral angles Ni–N(5)–C(20)–C(19)···N(4)–Ni(1)–N(5)–C(20) of 100(1), −75(1), 51(1), −75(1), 100(1), −43(1) and 43(1)°, respectively. The 1-Ph and 3-Ph substituents are twisted in respect to the parent pyrazole rings so that the dihedral angles are N(3)–N(2)–C(2)–C(7), 43(1), N(3)–C(8)–C(9)–C(10) 57(1), N(6)–N(7)–C(30)–C(31) 39(1) and N(6)–C(23)–C(24)–C(29) 32(1)°. The bond lengths of the nickel atom with amide nitrogens, Ni–N(1) and Ni–N(8), 1.878(6), 1.868(5) Å, are 0.03–0.04 Å shorter than those with the imine nitrogens, Ni–N(4) and Ni–N(5), 1.912(5) and 1.914(5) Å, respectively. Similar values have been reported[4d] for [1,3-bis(2-imidobenzylideneimino)propane]nickel(II). The complex [NiL^6] was found to be diamagnetic in the solid state.

Electronic spectra

The electronic spectra of complexes CuL (Table 5) were recorded in dimethylformamide solution and showed for all the compounds a close resemblance in the position of the absorption assigned to the π–π^* transitions of the co-ordinated aldimine group (339–350 nm) and ligand-to-metal charge-transfer (l.m.c.t.) bands (375–440 nm). Two lower-energy bands were assigned to the d–d metal transitions which are considered to be very sensitive to the ligand-field strength and changes in molecular geometry and correspond to the $^2B_2 \longrightarrow {}^2A_1$ and $^2B_2 \longrightarrow {}^2E$ transitions in D_{2d} symmetry. Planar-to-tetrahedral distortions decrease the transition energy and result in a red shift of both bands. For example, for bis(salicylaldiminato)-copper(II) complexes the ligand-field bands for the nearly planar *N*-ethyl-substituted complex were reported[15] at 12 000 and 16 000 cm^{-1} whereas for pseudo-tetrahedral bis(*N*-isopropylsalicylideneaminato)- and bis(*N*-*tert*-butylsalicyl-ideneaminato)-copper(II) they were at 9000, 14000 and 9000, 13 500 cm^{-1}, respectively. Complexes [CuL^4]–[CuL^6] were found to follow this trend with enlarging of the polymethylene chain. For [CuL^4] (n = 2), the ligand-field band maxima were observed at 520 and 700 nm, at lower wavelengths than corresponding absorptions for [CuL^5] (n = 3), 564 and 860 nm. Further shift to the infrared occurs in the case of [CuL^6] (n = 4) with the high-energy d–d transition appearing at 600 nm. For this complex we did not observe a second d–d band perhaps due to its low intensity even at the highest accessible concentration *ca.* 10^{-3} mol dm^{-3}. In contrast to [CuL^4]–[CuL^6], the ligand-field spectra of [CuL^1] (n = 2) and [CuL^2] (n = 3) containing a 1-methyl instead of a 1-phenyl pyrazole substituent are very similar indicating only minor structural reorganization which is also consistent with the ESR data (see below).

Planar Schiff-base nickel(II) complexes usually show a single ligand-field band at 500–600 nm whereas tetrahedral species demonstrate a complicated feature in the near infrared at 900–

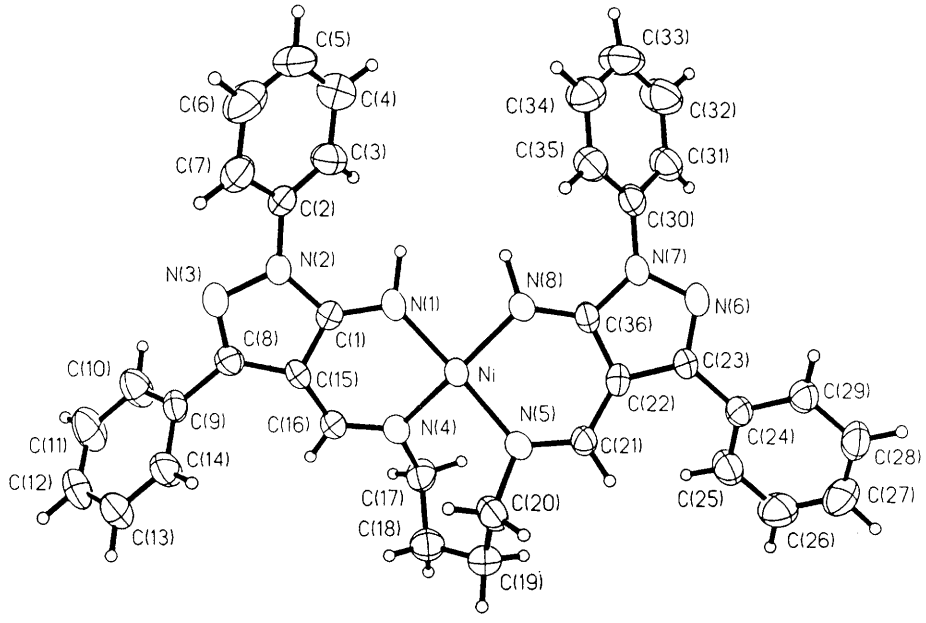

Fig. 1 Molecular structure of [NiL^6]

Table 3 Fractional atomic coordinates of the non-hydrogen atoms for the complex [NiL^6] with estimated standard deviations (e.s.d.s) in parentheses

Atom	*x*	*y*	*z*	Atom	*x*	*y*	*z*
Ni	0.0676(1)	0.4974(1)	0.2123(1)	C(24)	−0.1981(6)	0.6946(5)	0.4926(5)
N(1)	0.0881(5)	0.3718(4)	0.1851(4)	C(25)	−0.1892(7)	0.7849(5)	0.4286(5)
H(1N)	0.0367(5)	0.3041(4)	0.2184(4)	C(26)	−0.2131(8)	0.8714(6)	0.4599(7)
N(2)	0.1971(5)	0.2618(4)	0.0938(4)	C(27)	−0.2449(9)	0.8666(6)	0.5554(7)
N(3)	0.2789(5)	0.2726(4)	0.0075(4)	C(28)	−0.2542(7)	0.7768(6)	0.6200(6)
N(4)	0.1228(5)	0.5632(4)	0.0838(3)	C(29)	−0.2320(6)	0.6904(5)	0.5886(5)
N(5)	0.0908(5)	0.6151(4)	0.2560(3)	C(30)	−0.2439(6)	0.3523(5)	0.4875(4)
N(6)	−0.2384(5)	0.5205(4)	0.5053(4)	C(31)	−0.3810(7)	0.3410(5)	0.5102(5)
N(7)	−0.1889(5)	0.4474(4)	0.4595(4)	C(32)	−0.4359(8)	0.2480(6)	0.5363(7)
N(8)	−0.0308(5)	0.4351(4)	0.3252(4)	C(33)	−0.3564(9)	0.1648(6)	0.5392(7)
H(8N)	−0.059(5)	0.359(4)	0.332(4)	C(34)	−0.2228(8)	0.1766(6)	0.5159(6)
C(1)	0.1643(6)	0.3528(4)	0.1133(4)	C(35)	−0.1651(7)	0.2678(5)	0.4913(5)
C(2)	0.1655(6)	0.1664(5)	0.1506(5)	C(36)	−0.0971(6)	0.4839(5)	0.3843(4)
C(3)	0.0375(7)	0.1463(5)	0.1907(6)	C(37)	0.5901(9)	0.2427(7)	0.2573(7)
C(4)	0.0048(9)	0.0557(6)	0.2484(6)	C(38)	−0.313(1)	−0.0954(8)	0.1046(8)
C(5)	0.099(1)	−0.0172(6)	0.2649(6)	Cl(11)	0.5211(3)	0.2657(2)	0.1474(2)
C(6)	0.226(1)	0.0015(6)	0.2244(6)	Cl(12)	0.7407(3)	0.3081(2)	0.2415(2)
C(7)	0.2613(8)	0.0937(5)	0.1653(5)	Cl(13)	0.5888(9)	0.1123(6)	0.2990(8)
C(8)	0.2914(6)	0.3677(5)	−0.0260(4)	Cl(14)	0.645(2)	0.116(1)	0.277(1)
C(9)	0.3658(6)	0.4080(5)	−0.1205(4)	Cl(15)	0.626(2)	0.1254(9)	0.312(1)
C(10)	0.3319(7)	0.3846(6)	−0.2015(5)	Cl(41)	−0.4157(9)	−0.1290(5)	0.2180(5)
C(11)	0.4018(8)	0.4222(7)	−0.2878(5)	Cl(42)	−0.372(1)	0.0240(7)	0.0417(7)
C(12)	0.5064(7)	0.4829(6)	−0.2953(5)	Cl(43)	−0.153(1)	−0.119(1)	0.128(1)
C(13)	0.5395(7)	0.5082(6)	−0.2151(6)	Cl(44)	−0.345(2)	0.030(1)	0.070(1)
C(14)	0.4709(7)	0.4718(6)	−0.1277(5)	Cl(45)	−0.453(1)	−0.138(1)	0.191(1)
C(15)	0.2243(6)	0.4228(5)	0.0355(4)	Cl(46)	−0.147(2)	−0.067(2)	0.084(2)
C(16)	0.1882(6)	0.5236(4)	0.0197(4)	Cl(47)	−0.296(2)	0.019(1)	0.048(2)
C(17)	0.0724(7)	0.6652(5)	0.0459(5)	Cl(48)	−0.100(2)	−0.036(2)	0.035(2)
C(18)	0.1686(8)	0.7458(5)	0.0451(6)	Cl(49)	−0.170(2)	−0.082(2)	0.148(2)
C(19)	0.1833(8)	0.7681(5)	0.1403(5)	Cl(50)	−0.328(3)	−0.115(2)	0.216(2)
C(20)	0.2099(6)	0.6768(5)	0.2185(5)	Cl(51)	−0.158(2)	−0.140(1)	0.162(1)
C(21)	0.0201(5)	0.6414(5)	0.3265(4)	Cl(52)	−0.427(5)	−0.019(4)	0.056(3)
C(22)	−0.0821(6)	0.5849(5)	0.3832(4)	Cl(53)	−0.239(4)	−0.122(3)	0.206(2)
C(23)	−0.1735(6)	0.6009(5)	0.4606(4)				

1400 nm consisting of two or three components which may be assigned to $^3T_{1g} \longrightarrow {}^3T_{2g}$, $^3T_{1g}(F) \longrightarrow {}^3T_{1g}(P)$ and $^3T_{1g} \longrightarrow {}^3A_{2g}$ transitions.[16] Complexes [NiL^1]–[NiL^4] with n = 2–4 reveal very similar spectral patterns in $CHCl_3$ (Table 6) with a single ligand-field band at 583–615 nm consistent with planar geometry. Incorporation of the more flexible butane chain as in the case of [NiL^6] results in the presence of an amount of tetrahedral high-spin form. This is evidenced by the decrease in intensity of the ligand-field band at 600 nm and the appearance of two components of low intensity at 1038 and 1189 nm.

NMR spectra

Proton NMR spectra of complexes [NiL^1], [NiL^2], [NiL^4] and [NiL^5] with n = 2 or 3 display chemical shifts (Table 6) corresponding to a low-spin species with planar metal

configuration and similar to those observed for the free H_2L. The increase in length of the polymethylene strap to $n = 4$ in the case of [NiL^6] results in the appearance of large contact shifts characteristic of paramagnetic high-spin nickel(II) complexes (Fig. 2). The chemical shifts were independent of concentration ($c = 3 \times 10^{-2}$–5×10^{-3} mol dm^{-3}) and very similar in $CDCl_3$ and CD_2Cl_2 thus indicating the absence of intermolecular association in solution. The non-linear dependence of the contact shifts on $1/T$ (Table 7) indicates the occurrence of a planar $\rightleftharpoons$ tetrahedral equilibrium. The magnetic moments for [NiL^6] determined by the Evans method vary from 2.05 μ_B at 303 K to 2.23 μ_B at 331 K which corresponds to the proportion of the high-spin (h.s.) form, $N_{h.s.} = K/(1 + K)$ and equilibrium constant $K (= \mu_{expt}{}^2/\mu_{h.s.}{}^2$ where $\mu_{h.s.}$ is assumed to be 3.3 μ_B) of 0.385, 0.625, 0.450 and 0.838, respectively (Table 7). The thermodynamic parameters of the equilibrium ($\Delta G^\circ_{298} = 1.3 \pm 0.1$ kJ mol^{-1}, $\Delta H^\circ = 8.8 \pm 0.1$ kJ mol^{-1}, $\Delta S^\circ = 6 \pm 1$ J K^{-1} mol^{-1}) were obtained from standard equations as described previously.[16] At temperatures < 213 K the resonances of the NCH_2 group are represented by an AB spectrum consisting of two singlets perturbed by paramagnetic broadening [$\Delta\nu^\circ_{\frac{1}{2}} > {}^3J$(HH)] which coalesce at 213 K and transform to a four-proton singlet at elevated temperatures. The CCH_2 signals exhibit similar behaviour, coalescing at 229 K (Fig. 3).

Thus, at low temperatures a rapid (on the NMR time-scale) interconversion between low-spin planar and high-spin tetrahedral forms is not accompanied by $R \rightleftharpoons S$ racemization at the metal centre. The occurrence of eight spacial isomers forming four enantiomeric pairs is possible. These possess a tetrahedral T_R, T_S or planar P metal configuration and different conformations of the seven-membered metal ring, *viz.* twist-boat TB_r, TB_s and twist-chair TC_r, TC_s: P(TB_r)-P(TB_s), P(TC_r)-P(TC_s), $T_R(TB_r)$-$T_S(TB_s)$, $T_R(TC_r)$-$T_S(TC_s)$. At low temperatures the interconversion of enantiometric pairs is a slow process and the reaction pathways responsible for the $T(S = 1) \rightleftharpoons P(S = 0)$ rearrangements appear to be $T(TB) \rightleftharpoons P(TB)$ and $T(TC) \rightleftharpoons P(TC)$ interconversions proceeding with a retention of chirality at the metal centre and that of the metal ring.[17] At elevated temperatures the inversion of the seven-membered metal ring in [NiL^6] is apparently operative which at the same time involves inversion at the metal centre $T_R \rightleftharpoons T_S$. The representative reaction pathways at different temperatures are shown in Scheme 1. The activation barriers and rate constants for inversion at the coalescence temperatures were determined to be $\Delta G^\ddagger_{213} = 42.8$ [$k_{213} = 143.9$, $\Delta\nu = 64.8$ (NCH_2)] and $\Delta G^\ddagger_{229} = 44.2$ kJ mol^{-1} [$k_{229} = 339.6$ s^{-1}, $\Delta\nu = 180$ Hz (CCH_2)].

Table 4 Selected bond lengths (Å) and angles (°) for the complex [NiL^6] with e.s.d.s in parentheses

Ni–N(1)	1.878(6)	Ni–N(4)	1.912(5)
Ni–N(5)	1.914(5)	Ni–N(8)	1.868(5)
N(1)–H(1N)	1.074(8)	N(1)–C(1)	1.305(8)
N(2)–N(3)	1.410(7)	N(2)–C(1)	1.383(8)
N(2)–C(2)	1.416(8)	N(3)–C(8)	1.303(9)
N(4)–C(16)	1.304(8)	N(4)–C(17)	1.492(8)
N(5)–C(20)	1.483(8)	N(5)–C(21)	1.306(8)
N(6)–N(7)	1.393(8)	N(6)–C(23)	1.312(8)
N(7)–C(30)	1.403(9)	N(7)–C(36)	1.371(8)
N(8)–H(8N)	1.073(8)	N(8)–C(36)	1.331(8)
N(1)–Ni–N(4)	92.5(2)	N(1)–Ni–N(5)	164.2(2)
N(1)–Ni–N(8)	86.9(2)	N(4)–Ni–N(5)	91.7(2)
N(4)–Ni–N(8)	164.6(2)	N(5)–Ni–N(8)	93.1(2)
Ni–N(1)–H(1N)	129.5(5)	Ni–N(1)–C(1)	124.4(4)
H(1N)–N(1)–C(1)	106.0(6)	N(3)–N(2)–C(1)	111.2(5)
N(3)–N(2)–C(2)	120.3(5)	C(1)–N(2)–C(2)	128.4(5)
N(2)–N(3)–C(8)	105.4(5)	Ni–N(4)–C(16)	126.3(4)
Ni–N(4)–C(17)	119.0(4)	C(16)–N(4)–C(17)	114.1(5)
Ni–N(5)–C(20)	119.3(4)	Ni–N(5)–C(21)	125.9(4)
C(20)–N(5)–C(21)	114.1(5)	N(7)–N(6)–C(23)	105.0(5)
N(6)–N(7)–C(30)	119.3(5)	N(6)–N(7)–C(36)	112.0(5)
C(30)–N(7)–C(36)	128.4(5)	Ni–N(8)–H(8N)	117.3(5)
Ni–N(8)–C(36)	123.5(4)	H(8N)–N(8)–C(36)	116.5(6)

Table 5 UV/VIS spectral data for the CuL complexes

	λ_{max}/nm (log ε/dm^3 mol^{-1} cm^{-1})		
Complex	d–d	l.m.c.t.	π–π*
[CuL^1]	719 (2.14) 512 (sh) (2.25)	375 (3.86)	339 (3.14)
[CuL^2]	720 (2.18) 521 (sh) (2.27)	375 (3.86)	339 (3.85)
[CuL^4]	700 (2.28) 520 (sh) (2.48)	395 (3.65)	345 (3.95)
[CuL^5]	860 (2.44) 564 (sh) (2.61)	425 (3.44)	350 (4.09)
[CuL^6]	— 600 (2.56)	439 (3.98)	346 (3.97)

ESR spectra

The frozen-glass (dmf–MeOH) spectra of the copper(II) complexes (Fig. 4) have been analysed within the usual spin-Hamiltonian formalism[18] and the corresponding parameters are listed in Table 8. All the spectra are axial with $g_\parallel > g_\perp$. The ^{63,65}Cu hyperfine splitting $A_\parallel$ can be estimated directly from the spectra whereas $A_\perp$ was not resolved. In most cases the nitrogen superhyperfine structure is resolved on the low-field wing of the $g_\perp$ peak (eight to nine lines observed). The spectra suggest a common four-co-ordinate planar or pseudo-tetrahedral structure for all the complexes. A linear relation between variations in $A_\parallel$ and $g_\parallel$ values associated with planar-to-tetrahedral distortion at the metal centre in copper(II) complexes has been shown[19] for various chromophores. In the series of complexes [CuL^4]–[CuL^6] the values of $g_\parallel$ increase whereas $A_\parallel$ decrease on alteration of n from 2 to 4. If the complexes CuL can be related to those reported by Bereman *et al.*[19a] containing a CuN_2S_2 chromophore and assuming a similar shape of the plot of $g_\parallel$ or $A_\parallel$ *vs.* twist angle (corrected for

Table 6 Proton NMR and UV/VIS spectral data for the NiL complexes

		UV/VIS [λ_{max}/nm/log(ε/dm^3 mol^{-1} cm^{-1})]		
Complex	^{1}H NMR (δ, *J*/Hz)	d–d	l.m.c.t.	π–π*
[NiL^1]	2.20 (s, 6 H, $2CH_3$), 3.36 (s, 4 H, $2CH_2$), 7.24–7.40 [m, 14 H, 2(Ph, CHN and NH)]	595 (2.14)	438 (3.33)	390 (3.74)
[NiL^2]	1.88 (qnt, *J* 6.4, 2 H, CCH_2), 2.20 (s, 6 H, $2CH_3$), 3.65 (t, *J* 6.4, $2NCH_2$), 7.23–7.51 [m, 14 H, 2(Ph, CHN and NH)]	594 (2.19)	439 (3.48)	396 (4.02), 365 (3.91)
[NiL^4]	3.38 (s, 4 H, $2CH_2$), 7.28–7.66 [m, 24 H, 2(2Ph, CHN and NH)]	583 (2.05)	445 (3.25)	395 (3.65), 376 (3.54)
[NiL^5]	1.91 (qnt, *J* 6.5, 2 H, CCH_2), 3.61 (t, *J* 6.5, 4 H, $2NCH_2$), 7.27–7.66 [m, 24 H, 2(2Ph, CHN and NH)]	630 (2.15)		399 (3.68)
[NiL^6]	3.36 (s, 4 H, $2CCH_2$), 6.86 (t, *J* 7, 4 H, 2*m*-H), 7.32–7.36 (m, 6 H, 4*o*-H and 2*p*-H), 7.49 (t, *J* 7, 2 H, 2*p*-H), 7.78 (t, *J* 7, 4 H, 4*m*-H), 8.13 (d, *J* 7, 4 H, 4*o*-H), 29.40 (s, 2 H, 2NH), 45.90 (s, 4 H, $2NCH_2$), 107.15 (s, 2 H, 2CHN)	1189 (1.08), 1038 (0.89), 600 (2.29)	505 (2.83)	397 (3.74)

Table 7 Temperature dependence of the chemical shifts, magnetic moments and equilibrium constants for [NiL^6] in $CDCl_3$ [a]

						δ(^{1}H)		
T/K	$\Delta\nu$[b]/Hz	χ_m[c]	μ_{eff}/μ_B	$N_{h.s.}$[b]	K[e]	NCH_2	CH	NH
331	63.0	1866.2	2.23	0.45	0.84	50.5	120.9	33.0
323	60.8	1824.4	2.18	0.435	0.77	48.1	114.8	31.4
313	57.5	1761.8	2.11	0.41	0.70	45.9	107.1	29.4
303	54.9	1712.8	2.05	0.385	0.62	42.1	99.5	27.4
213[f]						14.9	30.7	9.2

[a] c = 41.24 mmol dm^{-3}. [b] Chemical shift difference for the reference hexamethyldisiloxane signal. [c] Molar susceptibility including Pascal corrections. [d] Fraction of the high-spin form. [e] Equilibrium constant for the planar ⟷ tetrahedral equilibrium. [f] Recorded in CD_2Cl_2.

Table 8 The EPR data for the CuL complexes

Complex	n	$g_{\|}$	$g_{\perp}$	$10^4A_{\|}$/cm^{-1}	10^4A_N/cm^{-1}
[CuL^1]	2	2.18	2.04	200	17
[CuL^2]	3	2.17	2.05	197	18
[CuL^4]	2	2.15	2.04	208	—
[CuL^5]	3	2.16	2.04	189	15
[CuL^6]	4	2.18	2.05	166	—

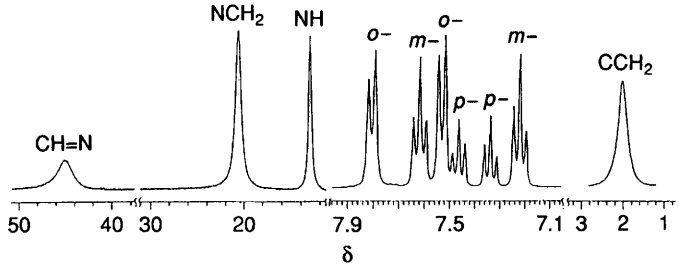

Fig. 2 Proton NMR spectrum of [NiL^6] at 263 K

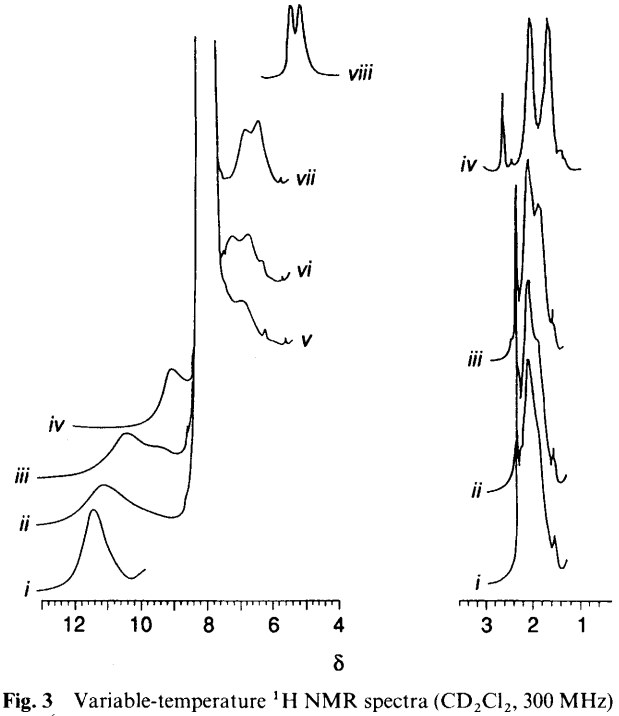

Fig. 3 Variable-temperature ^{1}H NMR spectra (CD_2Cl_2, 300 MHz) of [NiL^6] in the NCH_2 (*a*) and CCH_2 (*b*) regions: (*a*) 233 (*i*), 229 (*ii*), 226 (*iii*), 223 (*iv*), 213 (*v*), 210.5 (*vi*), 208 (*vii*) and 186 K (*viii*); (*b*) 213 (*i*), 210.5 (*ii*), 208 (*iii*) and 189 K (*iv*)

the higher values of the ESR parameters in the case of CuL), then the twist angle between the N(1)NiN(4) and N(5)NiN(8) planes can be roughly estimated to be 20([CuL^4], n = 2), 40([CuL^5], n = 3) and 55° ([CuL^6], n = 4).

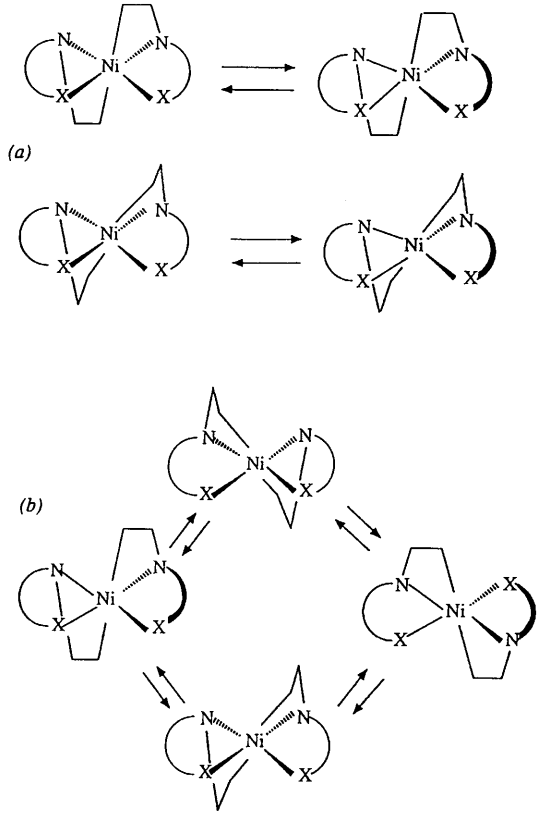

Scheme 1 Plausible rearrangement modes for the complex [NiL^6] at low (*a*) and high temperatures (*b*) (X = NH)

Cyclic voltammetry

Cyclic voltammetry of the CuL complexes in dimethylformamide revealed a complicated pattern of reversible and irreversible processes at different scan rates from 0.1 to 0.01 V s^{-1}. We assigned the peaks at *ca.* −1 V to irreversible $Cu^{II} \longrightarrow Cu^{I}$ reduction.[20] Under similar experimental conditions the NiL complexes display a quasi-reversible $Ni^{II} \longrightarrow Ni^{III}$ oxidation in contrast to the irreversible oxidation reported[21] for acetylacetone iminato complexes of Ni^{II}. The corresponding $E_{\frac{1}{2}}$ values are listed in Table 9. Stability of the electrochemically generated $Ni^{III}L$ species and the rather low $E_{\frac{1}{2}}$ values indicate a close analogy of the open-chain NiL complexes to their tetraaza macrocyclic counterparts. The main factors affecting the redox properties of the macrocyclic ligand complexes are considered[22] to be the presence of charge on the ligand, macrocyclic ring size and the nature of the ligand unsaturation. The negative charge on the ligand facilitates formation of the nickel(III) oxidation state at less negative potentials. The magnitude of $E_{\frac{1}{2}}$ *ca.* 0.5 V determined for the NiL complexes is higher than for corresponding macrocyclic species containing deprotonated ligands, $E_{\frac{1}{2}}$ < 0.3 V, whereas it is lower compared to those containing neutral ligands, $E_{\frac{1}{2}}$ > 0.6 V. The striking stabilization of Ni^{III} in macrocyclic complexes is accounted for by the

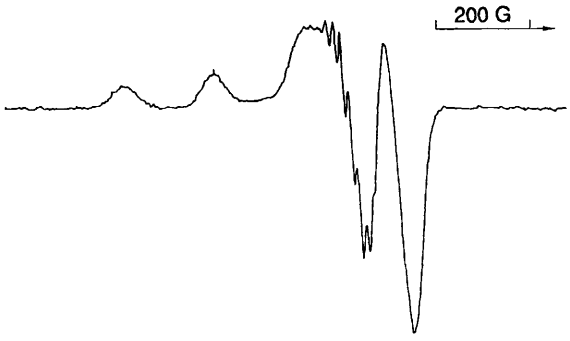

Fig. 4 X-Band ESR spectrum of [CuL^5] in dmf–MeOH at 77 K; G = 10^{-4} T

Table 9 Cyclic voltammetry data for the NiL complexes

Complex	$E_{\frac{1}{2}}$/V	ΔE/V	i_p^c/i_p^a
[NiL^1]	0.49	0.05	0.83
[NiL^2]	0.47	0.08	0.81
[NiL^4]	0.49	0.09	0.94
[NiL^5]	0.46	0.04	0.46
[NiL^6]	0.51	0.07	0.36

presence of the strong in-plane ligand field increasing the energy of the $d_{x^2-y^2}$ orbital so that removal of the electron from this orbital is essentially facilitated and occurs at less-positive potentials. We did not observe any pronounced dependence of the redox potentials for NiL on the length of the polymethylene chain even in the case of [NiL^6] ($n = 4$) possessing an apparently lower ligand field compared to that in the complexes with $n = 2$ or 3.

Acknowledgements

We are grateful to Dr. J. Becher for helpful discussions on the preparation of H_2L and to Dr. R. Hazell for preliminary data on the crystal structure determination.

References

1 A. D. Garnovskii, A. L. Nivorozhkin and V. I. Minkin, *Coord. Chem. Rev.*, 1993, **126**, 1.
2 H. Weigold and B. D. West, *J. Chem. Soc. A*, 1967, 1310; M. Hariharan and F. L. Urbach, *Inorg. Chem.*, 1969, **8**, 556; W. C. Hoyt and G. W. Everett, *Inorg. Chem.*, 1969, **8**, 2013; G. M. Mockler, G. W. Chaffey, E. Sinn and H. Wong, *Inorg. Chem.*, 1972, **11**, 1308; G. V. Panova, N. K. Vikulova and V. M. Potapov, *Russ. Chem. Rev.*, 1980, **49**, 655.
3 E. M. Martin, R. D. Bereman and P. Singh, *Inorg. Chem.*, 1991, **30**, 957; E. M. Martin and R. D. Bereman, *Inorg. Chim. Acta*, 1991, **188**, 221, 233; L. Casella, M. Gullotti, A. Pintar, F. Pinciroli and R. Vigano, *J. Chem. Soc., Dalton Trans.*, 1989, 1979; A. L. Nivorozhkin, L. E. Konstantinovsky, L. E. Nivorozhkin, V. I. Minkin, T. G. Takhirov, O. A. Diachenko and D. B. Tagiev, *Izv. Akad. Nauk SSSR, Ser. Khim.*, 1990, 327 (*Engl. Transl.*, 1990, 271); H. Frydendahl, H. Toftlund, J. Becher, J. C. Dutton, K. S. Murray, L. F. Taylor, O. P. Anderson and E. R. T. Tiekink, *Inorg. Chem.*, 1995, **34**, 4467.
4 (*a*) J. Weber, *Inorg. Chem.*, 1967, **6**, 258; (*b*) M. Green and P. A. Tasker, *J. Chem. Soc. A*, 1970, 2531; (*c*) B. M. Higson and E. D. McKenzie, *J. Chem. Soc., Dalton Trans.*, 1972, 269; (*d*) N. A. Bailey, E. D. McKenzie and J. M. Worthington, *J. Chem. Soc., Dalton Trans.*, 1974, 1363; (*e*) G. A. Bowmaker, T. N. Waters and P. E. Wright, *J. Chem. Soc., Dalton Trans.*, 1975, 867.
5 S. Knapp, T. P. Keenan, X. Zhang, R. Fikar, J. A. Potenza and H. J. Schugar, *J. Am. Chem. Soc.*, 1990, **112**, 3452; T. Pandiyan, M. Palaniandavar, M. Lakshminarayanan and H. Manohar, *J. Chem. Soc., Dalton Trans.*, 1992, 3377.
6 W. M. Davis, A. Zask, K. Nakanishi and S. J. Lippard, *Inorg. Chem.*, 1985, **24**, 3737.
7 W. M. Davis, M. M. Roberts, A. Zask, K. Nakanishi, T. Nozoe and S. J. Lippard, *Inorg. Chem.*, 1985, **24**, 3864.
8 D. F. Evans, *J. Chem. Soc.*, 1959, 2003; S. K. Sur, *J. Magn. Reson.*, 1989, **82**, 169.
9 E. A. Boudreaux and L. N. Mulay, in *Theory and Application of Molecular Paramagnetism*, Wiley, New York, 1976, pp. 491–495.
10 J. Becher, K. Pluta, N. Krake, K. Brøndum, N. J. Christensen and M. V. Vinader, *Synthesis*, 1989, 530.
11 P. L. Jørgensen, *Specialeraport*, Odense University, 1991.
12 (*a*) N. Walker and D. Stuart, *Acta Crystallogr., Sect. A*, **39**, 158; (*b*) G. M. Sheldrick, SHELXS 86, Program for Crystal Structure Determination, University of Göttingen, 1986; (*c*) G. M. Sheldrick, SHELXL 93, Program for Crystal Structure Refinement, University of Göttingen, 1993.
13 P. Caluwe, *Tetrahedron*, 1980, **36**, 2359.
14 I. Ya. Kvitko, L. V. Alam, N. I. Rtishchev, A. V. Eltsov, L. N. Kurkovskaya and N. B. Chebotareva, *Zh. Obshch. Khim.*, 1982, **52**, 2300.
15 R. Knoch, A. Wilk, R. Wannowius, D. Reinen and H. Elias, *Inorg. Chem.*, 1990, **25**, 3799.
16 R. H. Holm and M. J. O'Connor, *Prog. Inorg. Chem.*, 1971, **14**, 214.
17 M. J. O'Connor, R. E. Ernst and R. H. Holm, *J. Am. Chem. Soc.*, 1968, **90**, 4561.
18 J. R. Pilbrow, *Transition Ion Electron Paramagnetic Resonance*, Oxford University Press, 1990.
19 (*a*) R. D. Bereman, J. R. Dorfman, J. Bordner, D. P. Rillema, P. McCarthy and G. D. Shields, *J. Inorg. Biochem.*, 1982, **16**, 47; (*b*) A. Addison, in *Copper Coordination Chemistry. Biochemical and Inorganic Perspectives*, eds. K. D. Carlin and J. Zubieta, Adenine Press, New York, 1983; (*c*) H. Toftlund, J. Becher, P. H. Olesen and J. Z. Pedersen, *Isr. J. Chem.*, 1985, **25**, 56.
20 Y. Nishida, K. Unoura, T. Yokornizo and Y. Kato, *Inorg. Chim. Acta*, 1991, **181**, 141.
21 A. Kotočova, D. Valigura and J. Sima, *J. Coord. Chem.*, 1991, **24**, 363.
22 L. F. Lindoy, *The Chemistry of Macrocyclic Ligand Complexes*, Cambridge University Press, Cambridge, 1990.

Received 30*th August* 1995; *Paper* 5/05733G